Current Biology, Volume *33*

Supplemental Information

Epithelial apoptotic pattern emerges from global and local regulation by cell apical area

Victoire M.L. Cachoux, Maria Balakireva, Mélanie Gracia, Floris Bosveld, Jesús M. López-Gay, Aude Maugarny, Isabelle Gaugué, Florencia di Pietro, Stéphane U. Rigaud, Lorette Noiret, Boris Guirao, and Yohanns Bellaïche

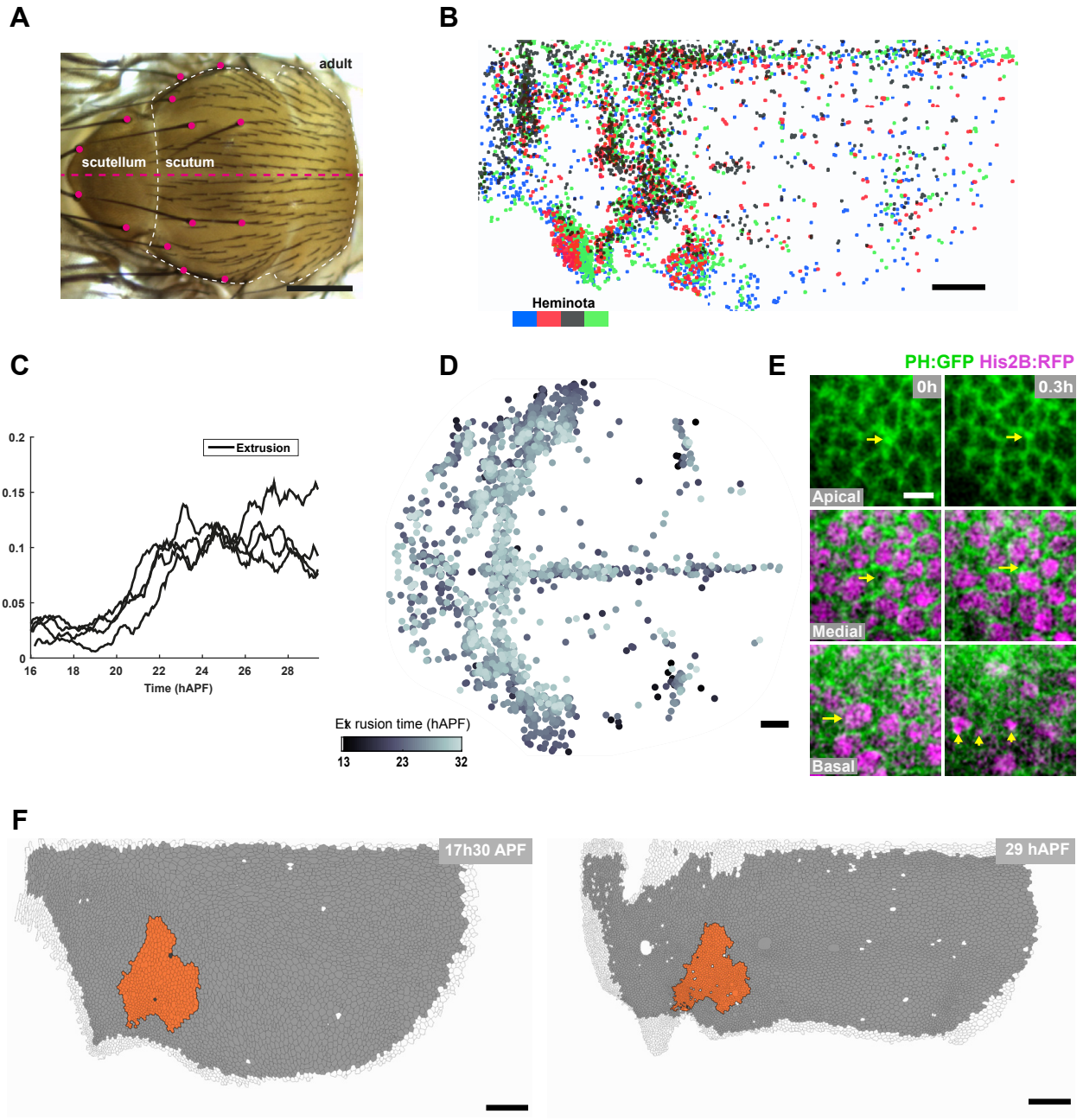
A
adult
scutellum
scutum
B
Heminota
C
Extrusion
Probability Distribution
0.2
0.15
0.1
0.05
0
16
18
20
22
24
26
28
Time (hAPF)
D
Ek rusion time (hAPF)
13
23
32
E
PH:GFP His2B:RFP
0h
0.3h
Apical
Medial
Basal
F
17h30 APF
29 hAPF

Figure S1. Adult notum and spatiotemporal patterns of cell apoptosis. Related to Figure 1 and Figure 2.

(**A**) *Drosophila* adult notum. Magenta dotted line: a-p axis. Magenta dots: macrochaetes. Dashed white line highlights scutum boundaries.

(**B**) Overlay of the spatial distributions of extrusions in 4 heminota (shown in blue, red, green, and black) between 15 and 29 hAPF and registered using the macrochaetae and the a-p axis as landmarks.

(**C**) Distributions of the extrusions as function of the developmental time in the 4 heminota shown in (B). On average, we record 850 ± 180 extrusions per heminota. The area under each curve is set to one.

(**D**) Map of the spatiotemporal distribution of extrusions in the notum. Dots indicate the extrusion positions color-coded according to their time of extrusion between 13h and 32 hAPF.

(**E**) Time-lapse images of PH:GFP and His2B:RFP in an apoptotic cell in the notum at the apical, medial and basal cell levels at the time of apical cell extrusion and 0.3 h later. Yellow arrows: position of the apoptotic cells. Yellow arrowheads: condensed His2B:RFP signal.

(**F**) Segmented Ecad:GFP notum highlighting tracked region 4 (shown in Figure 2) in orange at 17h30 APF (left) and 29 hAPF (right). Other cells are displayed in grey when they (or their progeny) could be tracked throughout the movie, otherwise they are displayed in white.

Scale bar: 50 μm (A,B,D,F), 5 μm (E).

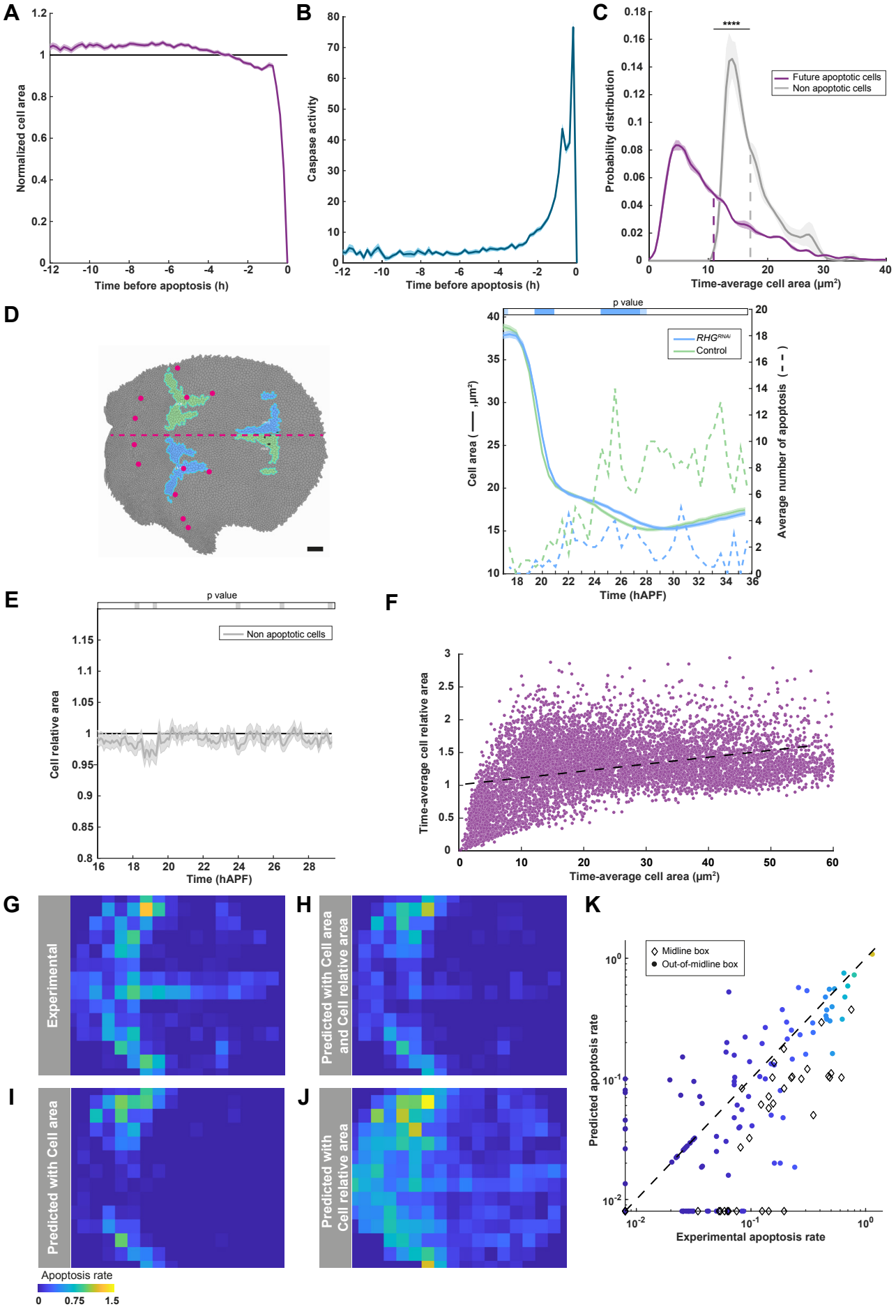
A
Normalized cell area
Time before apoptosis (h)
B
Caspase activity
Time before apoptosis (h)
C
****
Future apoptotic cells
Non apoptotic cells
Probability distribution
Time-average cell area (μm²)
D
p value
RHG^RNAi
Control
Cell area (—, μm²)
Average number of apoptosis (- - -)
Time (hAPF)
E
p value
Non apoptotic cells
Cell relative area
Time (hAPF)
F
Time-average cell relative area
Time-average cell area (μm²)
G
Experimental
H
Predicted with Cell area and Cell relative area
I
Predicted with Cell area
J
Predicted with Cell relative area
Apoptosis rate
0
0.75
1.5
K
Midline box
Out-of-midline box
Predicted apoptosis rate
Experimental apoptosis rate

Figure S2. Apical cell area and apoptosis. Related to Figure 3.

(**A**) Graph of the normalized apical area of the apoptotic cells (mean ± SEM) versus time before their apical extrusion. Time-evolutions of normalized areas of single cells have been aligned to their time of apical extrusion set to 0 h, then averaged. Every cell area is normalized to its average area during the first two hours of the cell's life. n = 2537 cells from N = 5 heminota.

(**B**) Graph of the Caspase activity of extruding cells (mean ± SEM) versus time before their extrusion. Caspase-activity is measured as the derivative of the GC3Ai signal as previously done [S1]. Time-evolutions of Caspase levels of single cells have been aligned to their time of apical extrusion set to 0 h, then averaged. n = 2537 cells from N = 5 heminota.

(**C**) Distributions of apical areas of future apoptotic cells averaged from the beginning of their life to 3h prior to their apical extrusion (purple, mean ± SEM) and apical areas of all cells of the tissue taken at same similar time points as the apoptotic cells (grey, mean ± SEM). Curves are smoothed over 3 data points. The area below each curve is one. n = 2599 cells from N = 4 heminota. Future apoptotic cells are on average 38% smaller than non-apoptotic cells, $p < 2.2 \times 10^{-42}$, Student's t-test.

(**D**) Left: Segmented notum with the RHG^{RNAi} clones (marked Caax:tBFP, not shown) outlined in blue and the control contralateral symmetric clones of cells in green. Magenta dashed line: a-p axis. Magenta dots: macrochaetae. Right: Graph of cell apical areas (blue, mean ± SEM) and of the number of cell extrusion (dotted blue line) in RHG^{RNAi} clones as well as in control contralateral symmetric cells (cell apical area, green, mean ± SEM, number of cell extrusion, dotted green line). n = 5943 RHG^{RNAi} cells and n = 6729 control cells from N = 2 heminota. Horizontal bar: p values of Student's t-tests comparing the cell apical areas in RHG^{RNAi} clones and control every 15 minutes, color-coded according to the p value (white, $p \geq 0.05$; light blue, $p < 0.05$; dark blue, $p < 0.01$).

(**E**) Graph of the relative apical areas of non-apoptotic cells (gray, mean ± SEM) within the apoptotic mask versus developmental time. n = 2536 cells randomly picked from N = 4 heminota. Horizontal bar: p values of Student's t-tests comparing the experimental curve and the reference average of 1 every 15 minutes color-coded according to the p value (white, $p \geq 0.05$; light grey, $0.01 < p < 0.05$).

(**F**) Graph of the relative apical cell areas versus apical cell areas, both quantities averaged over cell lives except for their last hour (before either extrusion or division). Dashed black line: linear fit, $R^2 = 0.15$. n = 8460 cells from N = 4 heminota.

(**G-J**) Coarse-grained maps of the experimental apoptosis rate corresponding to Figure 3F-I (G) and predicted apoptosis rates using both the area and relative area (H), the area only (I) or the relative area only (J) in the notum, and corresponding to Figures 3G-I. The color-coded apoptosis rates are calculated in each box as the number of apoptoses that occurred within the box, divided by the initial number of cells in the box. Box size: 40×40 μm².

(**K**) Predicted versus experimental apoptosis rates, for each box of the grid used in (H) and (G). Log-scale. White diamonds: midline boxes, (i.e., overlapping with the midline). Colored dots: non-midline boxes, color-coded as a function of the apoptotic rate (same color code as G). Dashed black line: y = x. Root Mean Square Error = 0.10 when including all boxes, 0.08 when excluding the midline boxes.

Scale bar: 50 μm. ****: $p<0.0001$. Clone induction regimes are described in Methods.

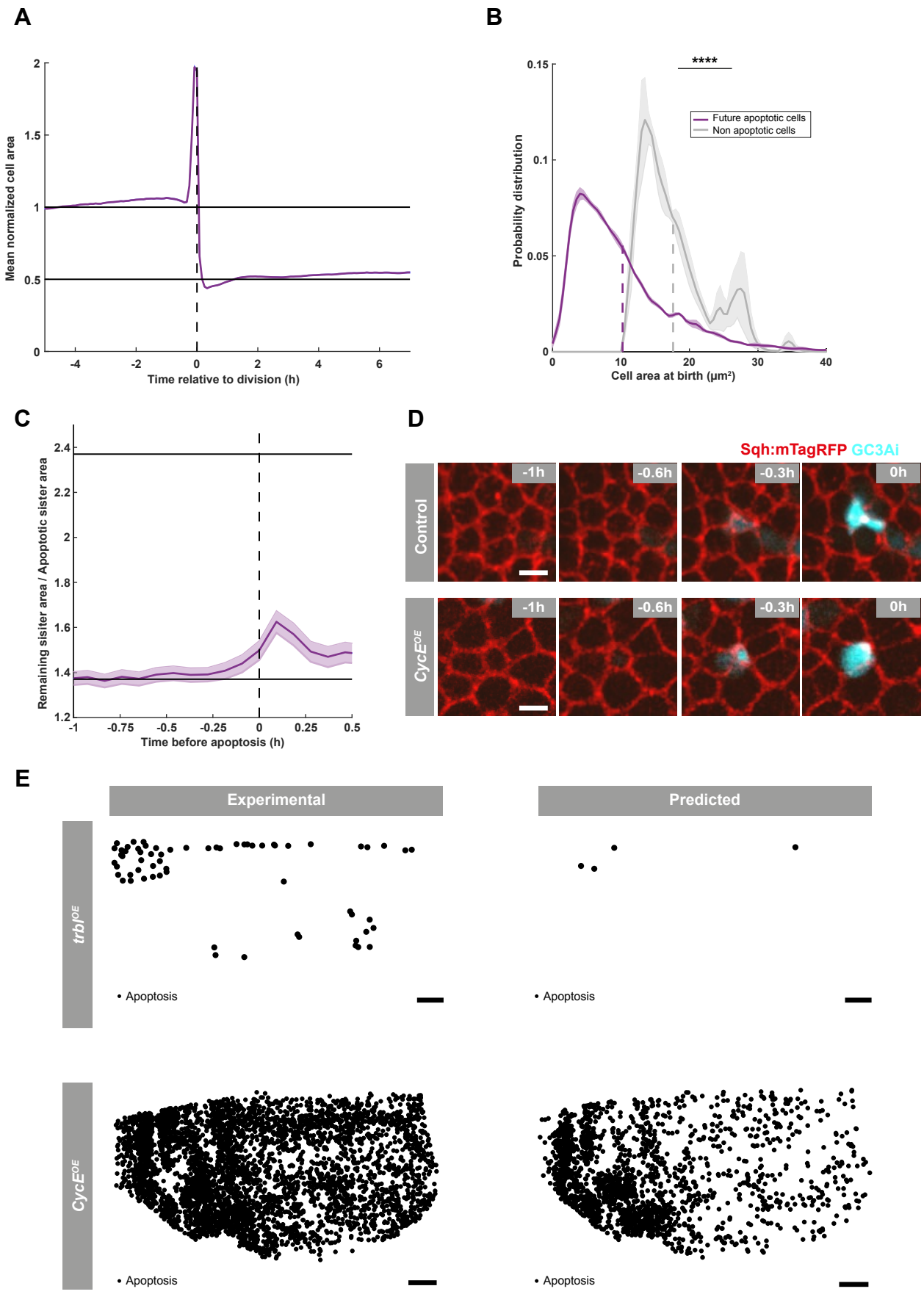
A
Mean normalized cell area
Time relative to division (h)
B
****
Future apoptotic cells
Non apoptotic cells
Probability distribution
Cell area at birth (µm²)
C
Remaining sisiter area / Apoptotic sister area
Time before apoptosis (h)
D
Sqh:mTagRFP GC3Ai
Control
CycE^OE
-1h
-0.6h
-0.3h
0h
E
Experimental
Predicted
trbl^OE
CycE^OE
• Apoptosis

Figure S3. Cell division and apoptosis in the notum. Related to Figure 4.

(**A**) Normalized apical area of non-apoptotic cells over time through division (mean ± SEM). Time is set to 0 at cytokinesis (formation of the Ecad positive daughter-daughter cell interface). Mother cells are tracked up to 5 h before cytokinesis, and their daughters up to 7 h after their births. Mother cell areas are normalized by their initial areas (averaged between -5 and -4 h). Daughter areas are renormalized by this same area so they can be compared to their respective mothers, and averaged between sister cells. The substantial variation of area occurs during cell division due to mitotic cell rounding. Despite the average daughter cell apical expansion after division that amounts to 9.5 ± 0.8% 7 hours after cytokinesis and right before their next division (taking 0.5 as initial mean daughter normalized area), the average cell apical area substantially decreases by 49 ± 0.5 % with each division round, (comparing mean cell area at -1h and +6h after division, since the distribution of cell cycle durations peaks at 7h). n = 6180 cells from N = 2 heminota.

(**B**) Distributions of apical areas of future apoptotic cells at the beginning of their life (area is averaged up to 1h30 after the division of their mother, purple, mean ± SEM) and apical areas of all cells of the tissue taken at same similar time point as the apoptotic cells (grey, mean ± SEM). Curves are smoothed over 3 data points. The area below each curve is one. n = 4244 cells from N = 4 heminota. Future apoptotic cells are on average 42% smaller than non-apoptotic cells, p = 0 (too small to be computed), Student's t-test.

(**C**) Time evolution of the area of the surviving sister cell in pairs of surviving/apoptotic sister cells, normalized by the area of its apoptotic sister 1h prior to its extrusion (mean ± SEM). On average, the surviving sister cell is 1.37 times larger than its apoptotic counterpart 1h before extrusion (bottom horizontal line). During the apoptosis of its sibling, this normalized sister cell area increases by at most 0.25, indicating that the surviving sister cell transiently grows by 25% of the size its sibling occupied 1h before extrusion. An increase to 2.37 (top horizontal line) would mean that the surviving sister cell has completely occupied the space vacated by its apoptotic sibling. Time is set to zero at the moment of the apoptotic sister cell's extrusion. n = 690 cells from N = 4 heminota.

(**D**) Time-lapse images of Sqh:mTagRFP and the GC3Ai Caspase reporter in extruding cells in control (top) and $CycE^{OE}$ (bottom) nota. In control notum, 91 % of the extruding cells (n = 160 cells in N = 2 nota) are GC3Ai positive. Upon overexpression of CycE, 88% of the extruding cells (n = 239 cells in N = 2 nota) accumulate GC3Ai signal during extrusion. Time (h) is set to 0 at the time of apical extrusion.

(**E**) Experimental (left) and predicted (right) spatial maps of apoptosis in $trbl^{OE}$ (top, F1-score = 0.29) and $CycE^{OE}$ (bottom, F1-score = 0.54) heminota, using both the area and relative area. Black dots indicate the positions of the experimental or predicted apoptoses. F1-score for a random model: 0.14.

Scale bars: 5 µm (C), 50 µm (D). ****: $p<0.0001$.

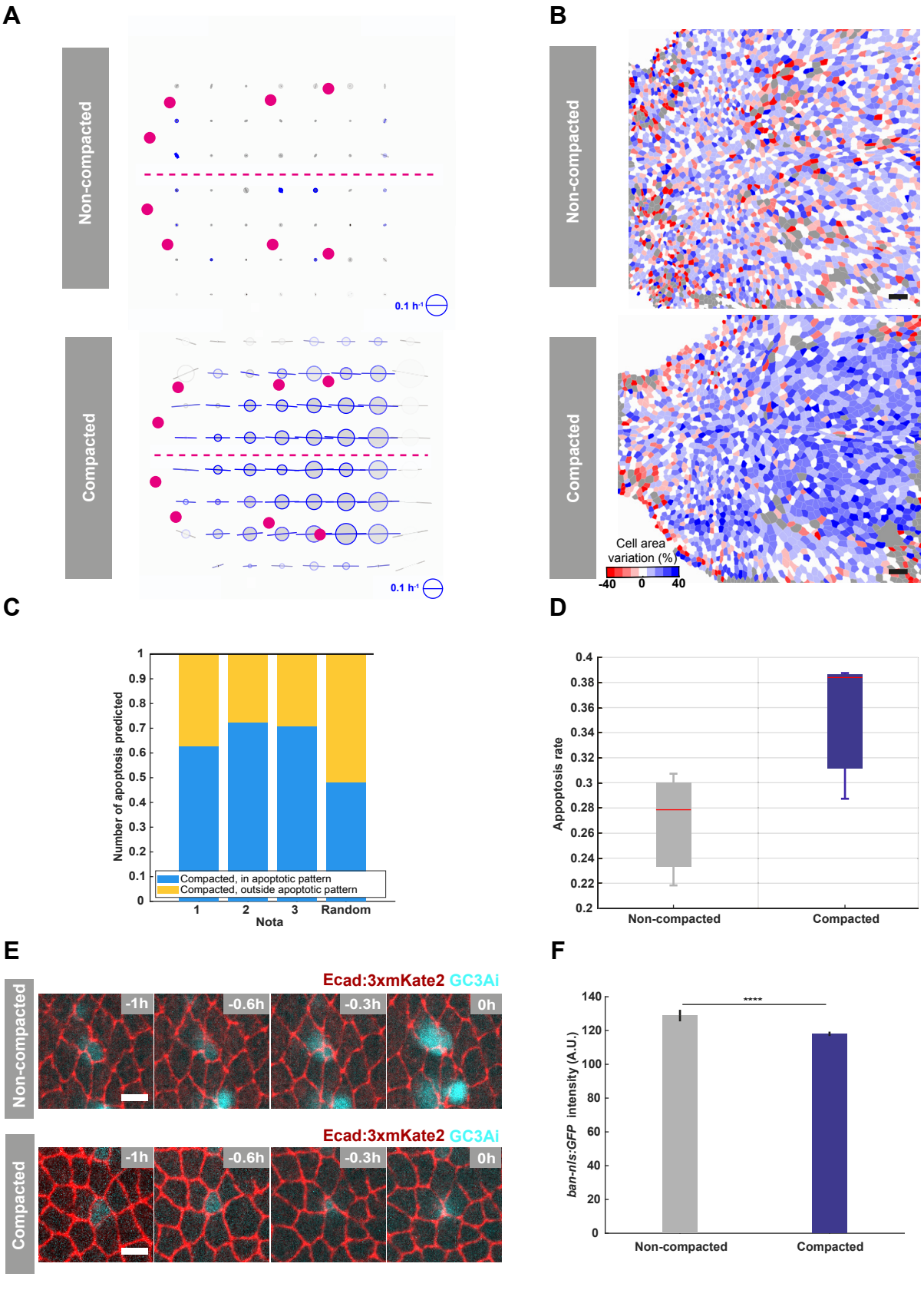
A
Non-compacted
0.1 h⁻¹
Compacted
0.1 h⁻¹
B
Non-compacted
Compacted
Cell area variation (%)
-40
0
40
C
Number of apoptosis predicted
Compacted, in apoptotic pattern
Compacted, outside apoptotic pattern
1
2
3
Random
Nota
D
Appoptosis rate
Non-compacted
Compacted
E
Ecad:3xmKate2 GC3Ai
Non-compacted
-1h
-0.6h
-0.3h
0h
Ecad:3xmKate2 GC3Ai
Compacted
-1h
-0.6h
-0.3h
0h
F
****
ban-nls:GFP intensity (A.U.)
Non-compacted
Compacted

Figure S4. Ectopic compaction and cell apoptosis. Related to Figure 5.

(**A**) Maps of tissue rate of deformation in non-compacted tissue averaged over 30 min (top, N = 3 nota), and in a compacted tissue over the 30 min compaction (bottom, N = 3 nota) in the posterior medial notum region. The grey disks indicate a pure decrease of area, whereas the bars quantify the pure change of shape (contraction-elongation or shear) and indicate the direction of elongation. Magenta dotted line: a-p axis. Magenta dots: macrochaetes.

(**B**) Color-coded segmented images representing the cell area relative variations between t = 0 and t = 30 min, in non-compacted (top) and compacted (bottom) pupal nota. The positive variations are coded in shades of red and the negative one in shades of blue, showing a decrease of the cell apical area after compaction. The dividing cell are colored in grey and are not considered because of their change in apical size due to division. Individual cell area relative variations over the 30 min of imposed compaction (as well as in non-compacted tissues), were then calculated as follows: (final area – initial area)/ initial area.

(**C**) Normalized number of compaction-induced additional apoptoses predicted to occur either inside (blue) or outside (yellow) the apoptotic mask, following a 19%-tissue compaction in 3 nota ("1" to "3") as well as the expected proportions in and out the apoptotic mask, if these apoptoses were randomly selected in the region ("random"). The total number of additional apoptoses is normalized to 1.

(**D**) Boxplot of the experimental apoptosis rate in non-compacted (grey) and compacted nota (blue). N=3 nota. The box represents the interquartile range (between the 1st and 3rd quartile). Each whisker represents respectively the maximum and the minimum values. The red line represents the median.

(**E**) Time-lapse images of Ecad:3xmKate2 and the GC3Ai Caspase reporter in extruding cells in non-compacted (top) and a compacted (bottom) nota. In non-compacted tissue, 81% of the extruding cells are GC3Ai positive (n=132 extruding cells in N=2 nota). In compacted tissue, 85% of the extruding cells were GC3Ai positive (n=114 extruding cells in N=2 nota). Time (h) is set to 0 at the time of apical extrusion.

(**F**) Graph of the *ban-nls:GFP* fluorescent intensity (mean over a given subregion) at 20h30APF in non-compacted (grey, n = 9 subregions per notum, N = 3 nota) and compacted nota (blue, n = 9 subregions per notum, N = 3 nota). Error bar: 95%-CI. $p = 1.4\times10^{-20}$, Mann-Whitney test.

Scale bars: 20µm (B), 5 µm (E). ****: $p<0.0001$

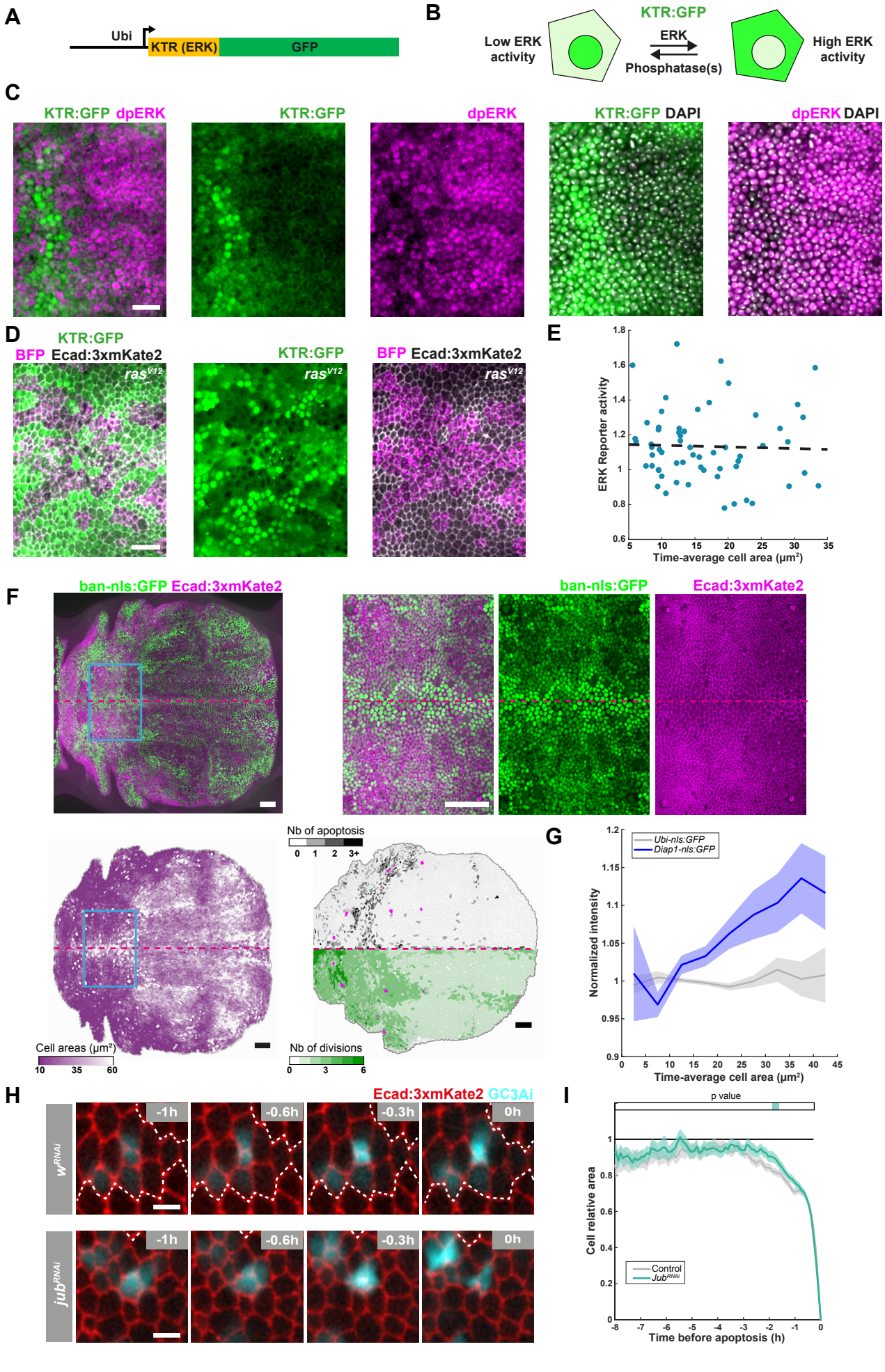
A
Ubi
KTR (ERK)
GFP
B
KTR:GFP
Low ERK activity
ERK
Phosphatase(s)
High ERK activity
C
KTR:GFP dpERK
KTR:GFP
dpERK
KTR:GFP DAPI
dpERK DAPI
D
KTR:GFP
BFP Ecad:3xmKate2
ras^V12
KTR:GFP
BFP Ecad:3xmKate2
ras^V12
E
ERK Reporter activity
Time-average cell area (µm²)
F
ban-nls:GFP Ecad:3xmKate2
ban-nls:GFP
Ecad:3xmKate2
Nb of apoptosis
0 1 2 3+
Cell areas (µm²)
10 35 60
Nb of divisions
0 3 6
G
Ubi-nls:GFP
Diap1-nls:GFP
Normalized intensity
Time-average cell area (µm²)
H
Ecad:3xmKate2 GC3Ai
w^RNAi
jub^RNAi
-1h
-0.6h
-0.3h
0h
I
p value
Cell relative area
Control
Jub^RNAi
Time before apoptosis (h)

Figure S5. ERK and Hippo/YAP signaling in apoptosis. Related to Figure 6.

(**A**) Schematic of the Ubi-KTR:GFP construct.

(**B**) Expected localization of KTR:GFP reporter as a function of ERK activity. In absence of ERK activity KTR:GFP localizes in the nucleus whereas KTR:GFP is enriched in the cytoplasm when ERK is active. The ratio between the GFP nuclear and cytoplasmic signal is used as a reporter of ERK activity [S2].

(**C**) KTR:GFP (green), dpERK (purple) and DAPI (white) localizations in the pupal notum at 24 hAPF. To validate the KTR:GFP reporter, the di-phosphorylated ERK (active) localization was compared to the one of KRT:GFP. KTR:GFP is localized in the nucleus in absence of dpERK nuclear localization, whereas KTR:GFP is mainly localized in the cytoplasm when dpERK signal is detected in the nucleus.

(**D**) KTR:GFP (green) and Ecad:3xmKate (white) localization in pupal notum harbouring clones overexpressing the activated ras^{V12} form (marked by Caax:BPF, purple). To further test whether KTR:GFP is localized in the cytoplasm upon ERK activation, the constitutive active ras^{V12} was expressed in clones and the localization of the KTR:GFP was compared inside and outside the ras^{V12} clones. KTR:GFP is mainly localized outside of the nucleus in ras^{V12} clones.

(**E**) ERK activity versus cell apical area notum. ERK activity and cell apical area are averaged over 30 minutes. Measurements are made at around 24 hAPF in the posterior medial region of the notum. Dashed line: linear fit, $p = 0.8$ and $R^2 = 0.0012$. n = 60 cells from N = 4 nota.

(F) Top: Pupal notum labeled by Ecad.3xmKate and ban-nls:GFP at 22h30APF (left), and close-up on the squared blue region (right panels). Bottom left: segmented image of the same notum where cells are color-coded according to their apical areas. Bottom right: segmented notum where cells are color-coded according to the upcoming number of apoptoses (up: left heminotum) or divisions (bottom: right heminotum) they or their progeny will undergo. Magenta dashed line: a-p axis. Magenta dots:macrochaetae (bottom right)

(G) Graph of Diap1-nls:GFP (blue) and Ubi-nls:GFP (grey) signal (mean ± SEM*)* versus cell apical areas. Diap-nls:GFP: n=1174 cells from N=2 nota. Ubi-nls:GFP: n = 1233 cells from N = 2 nota. Cells are binned in 5 µm²-wide bins from 0 to 45 µm². Data points are from [S3].

(**H**) Time-lapse images of Ecad:3xmKate2 and the GC3Ai Caspase reporter prior and during cells extrusion inside control (w^{RNAi}, top) and jub^{RNAi} (bottom) clones, marked by the accumulation of Caax:BFP (not shown) and outlined by a white dotted line. 95 % of the extruding cells (n = 233 cells in N = 3 nota) are GC3Ai positive in w^{RNAi} clones, while 90% of the extruding cells (n = 323 cells in N = 3 nota) accumulate GC3Ai signal during extrusion in jub^{RNAi} clones. Time (h) is set to 0 at the time of apical extrusion.)

(**I**) Relative apical area of apoptotic cells (mean ± SEM) versus time before their death in jub^{RNAi} (green, n = 284 cells from N = 4 nota) versus control contralateral symmetric (grey, n = 284) cells. Time-evolution of cells have been aligned to their time of apoptosis set to t = 0, and then averaged. Horizontal bar: p values of Student's t-tests comparing the relative area and an average of 1 every 15 minutes color-coded according to the p value (white, $p \geq 0.05$; light green, $0.01 < p < 0.05$).

Scale bars: 5 µm (C, D, E), 50 µm (F). Clone induction regimes are described in Methods.

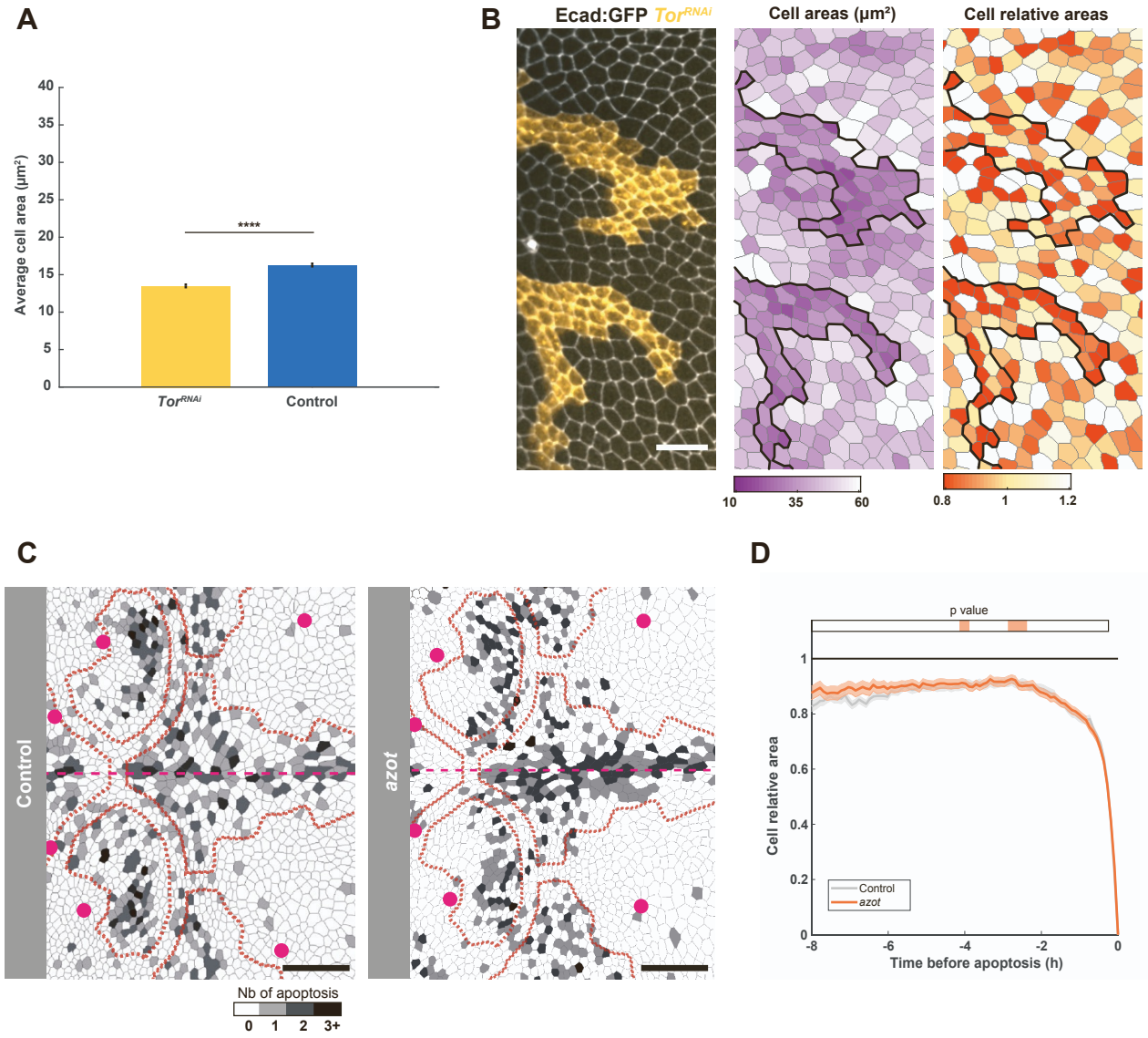
A
Average cell area (µm²)
40
35
30
25
20
15
10
5
0
****
Tor^RNAi
Control
B
Ecad:GFP Tor^RNAi
Cell areas (µm²)
Cell relative areas
10
35
60
0.8
1
1.2
C
Control
azot
Nb of apoptosis
0
1
2
3+
D
p value
1
0.8
0.6
0.4
0.2
0
Cell relative area
Control
azot
-8
-6
-4
-2
0
Time before apoptosis (h)

Figure S6. Cell relative area and apoptosis. Related to Figure 7.

(**A**) Graph of the apical areas in Tor^{RNAi} clone cells (yellow, mean ± SEM, n = 3640 cells from 10 clones in N = 2 nota) and in control cells (blue, n = 7798 cells). Control cells are made up by the R1 and R2 WT cells surrounding each Tor^{RNAi} clone (Figure 7A). The apical areas are averaged over the cells lives except for their last hour of existence when they underwent apoptosis or division. $p = 3 \times 10^{-27}$, Kolmogorov-Smirnov test.

(**B**) Left: close-up of a Ecad:GFP notum with a Tor^{RNAi} clone (yellow, marked by Caax:BFP) at 15 hAPF; Middle and Right: corresponding segmented image with cells color-coded according to their apical area (middle) or relative apical area (right).

(**C**) Apoptosis maps in control (left) and *azot* (right) tissues at 15 hAPF, with the apoptosis mask outlined by thick dashed red lines. Nota cells are color-coded according to the upcoming number of apoptosis in their progeny (white: no extrusion, black: at least 3 extrusions). Magenta dashed line: midline. Magenta dots: macrochaetae.

(**D**) Graph of the relative apical area of apoptotic cells (mean ± SEM) in the scutellum versus time before their death, in *azot* (orange, n = 533 cells from N = 2 nota) and WT (grey, n = 1198 cells from N = 4 nota) cells. Time-evolution of cells have been aligned to their time of apical extrusion set to t = 0, then averaged. Horizontal bar: p values of Student's t-tests performed between *azot* and the wt tissues every 15 minutes, and color coded according to the p value (white, $p \geq 0.05$; light orange, $0.01 < p < 0.05$).

Scale bars: 20 µm (B), 50µm (C). ****: $p<0.0001$. Clone induction regimes are described in Methods.

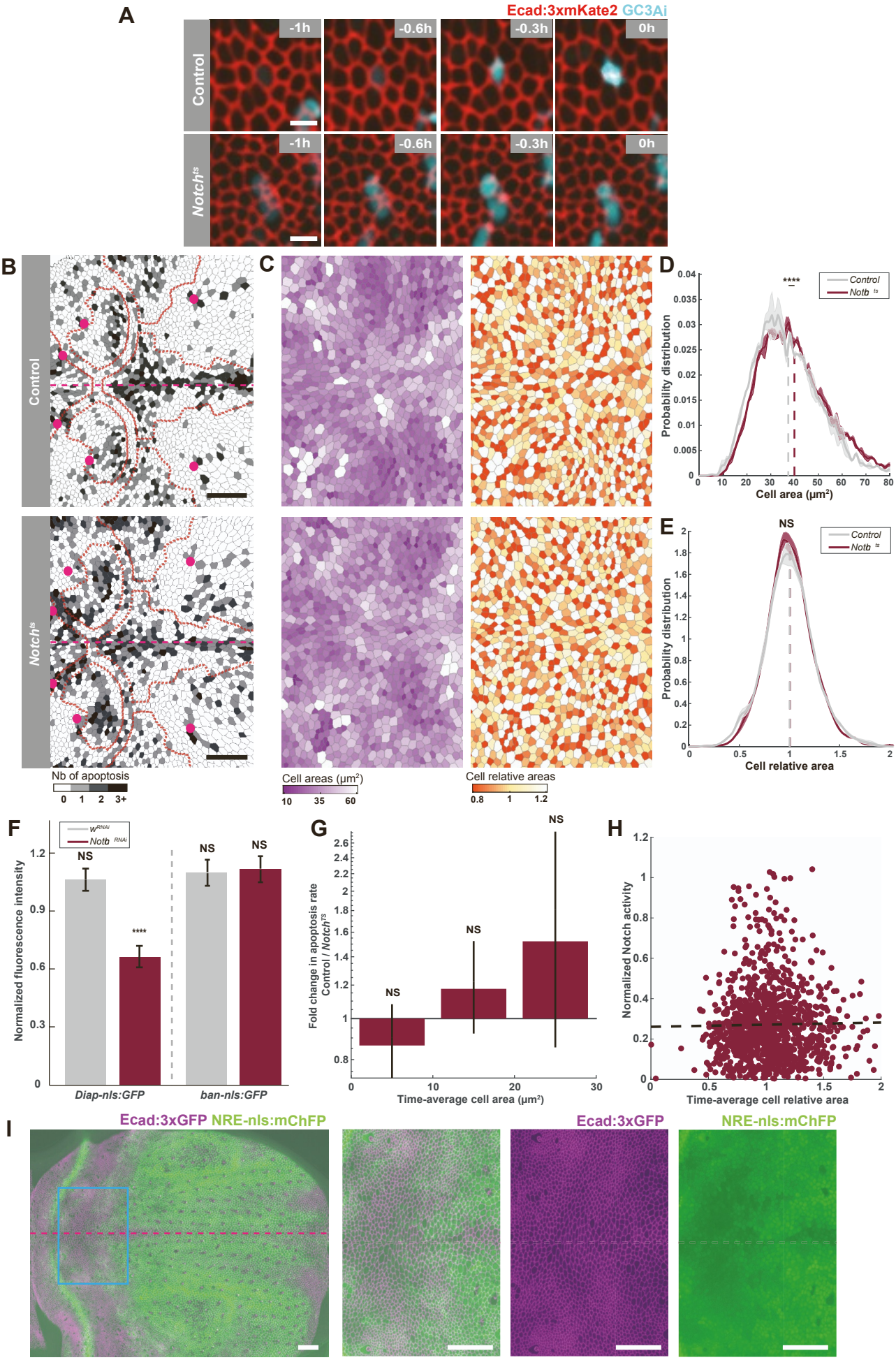
A
Ecad:3xmKate2 GC3Ai
Control
Notch^ts
-1h
-0.6h
-0.3h
0h
B
Control
Notch^ts
Nb of apoptosis
0 1 2 3+
C
Cell areas (µm²)
10 35 60
Cell relative areas
0.8 1 1.2
D
Control
Notb ts
****
Probability distribution
Cell area (µm²)
E
NS
Control
Notb ts
Probability distribution
Cell relative area
F
W RNAi
Notb RNAi
NS
****
NS
NS
Normalized fluorescence intensity
Diap-nls:GFP
ban-nls:GFP
G
NS
NS
NS
Fold change in apoptosis rate
Control / Notch^TS
Time-average cell area (µm²)
H
Normalized Notch activity
Time-average cell relative area
I
Ecad:3xGFP NRE-nls:mChFP
Ecad:3xGFP
NRE-nls:mChFP

Figure S7. Notch signaling in apoptosis. Related to Figure 7.

(**A**) Time-lapse images of Ecad:3xmKate2 and the GC3Ai Caspase fluorescence reporter prior and during cell extrusion in a control (top) and a *Notch^{ts}* (bottom) tissue. Time (h) is set to 0 at apical extrusion.

(**B**) Apoptosis maps in control (top) and *Notch^{ts}* (bottom) tissues at 15 hAPF, with the apoptosis mask outlined by thick dashed red lines. Nota cells are color-coded according to the upcoming number of apoptosis in their progeny (white: no extrusion, black: at least 3 extrusions). Magenta dashed line: midline. Magenta dots: macrochaetae.

(**C**) Segmented images of the nota shown in Figure S7B, in control (top) and *Notch^{ts}* (bottom) tissues at 15 hAPF, where cells are color-coded according to their apical areas (left) and relative area (right). Magenta dashed line: midline.

(**D-E**) Distributions of cell apical areas (D, mean ± SEM), and cell relative apical areas (E, mean ± SEM) of cells at 16 hAPF in control (gray, n = 4347 cells from N = 2 nota) and *Notch^{ts}* nota (dark red, n = 6482 cells from N = 3 nota). Curves are smoothed over 3 points. The area below each curve is set to one. Dashed lines: average values. Apical area, $p = 6.5 \times 10^{-19}$ and relative area, p = 0.53, Student's t-tests.

(**F**) Graph of the normalized *ban-nls:GFP* and Diap1-nls:GFP reporters (mean ± SEM) in *w^{RNAi}* and *Notch^{RNAi}* clones. Reporter levels were normalized by the contralateral symmetric control cells. *ban-nls:GFP*: n = 89 *w^{RNAi}* clones from N = 3 nota, p = 0.18 and n = 61 *Notch^{RNAi}* clones from N = 4 nota, p = 0.76; *Diap1-nls:GFP*: n = 39 *w^{RNAi}* clones from N = 3 nota, p = 0.63 and n = 36 *Notch^{RNAi}* clones from N = 3 nota, $p = 2.5 \times 10^{-6}$; Paired Wilcoxon-Mann-Whitney bilateral tests.

(**G**) Graph of the fold-change in apoptosis rate between control cells (n=1500 cells from N=2 nota) and *Notch^{ts}* cells (n=1500 cells from N=3 nota) versus cell apical area. Log-scale. Error bar: 95%-CI, Fisher test. For each condition, 1500 cells were randomly selected, a number comparable to the ones analyzed in *jub^{RNAi}* (Figure 6D) and *Actn^{RNAi}* (Figure 6E) conditions. p values: 0.22 (0-10 µm²), 0.23 (10-20 µm²), 0.16 (20-30 µm²), Fisher test.

(**H**) Graph of the normalized *NRE-nls:ChFP* reporter activity versus cell relative apical area (n = 1189 from N = 7 nota). A min-max normalization on the 0.1 and 99.9 percentiles was performed. Dashed black line: linear fit, $R^2 = 2.7 \times 10^{-4}$, p = 0.57.

(**I**) Left: Pupal notum labeled by Ecad:3xGFP and *NRE-nls:ChFP* reporter at 22h30 APF. Right: close-up of the squared blue line region. Magenta dashed line: a-p axis.

Scale bars: 5 µm (A), 50 µm (B,I). NS: $p \geq 0.05$; **: $p < 0.01$; ****: $p < 0.0001$. Clone induction regimes are described in Methods.

	Estimate β	Standard error	z	p value
Intercept	$\beta_0 = 1.01$	0.105	9.65	$< 5 \times 10^{-4}$ **
Cell apical area	$\beta_1 = -0.104$	0.003	-30.9	$< 5 \times 10^{-4}$ **
Cell Relative apical area	$\beta_2 = -1.91$	0.126	-15.1	$< 5 \times 10^{-4}$ **

Table S1. Multivariate logistic regression. Related to Figure 3.

The probability for a cell to enter apoptosis is modelled by the following equation on its apical geometry characteristics: Apoptosis $\approx \beta_0 + \beta_1 \times$ Area $+ \beta_2 \times$ Relative area, where the β_i values are given in the table. Significance: ** $p<0.01$. z-values: estimate divided by standard error. n = 30034.

Figure Panel	Genotype
1A	w; Ecad:GFP/ Ecad:GFP
1B	w; Ecad:GFP/ Ecad:GFP
1C	w; Ecad:GFP/ Ecad:GFP
1D	w; Ecad:GFP/ Ecad:GFP
1E	w; Ecad:3xmKate2/+; Act-Gal4, Ubi-GAL80^{ts} / UAS-GC3Ai
2A	w; Ecad:GFP/ Ecad:GFP
2B	w; Ecad:GFP/ Ecad:GFP
3A	w; Ecad:GFP/ Ecad:GFP
3B	w; Ecad:GFP/ Ecad:GFP
3C	w; Ecad:GFP/ Ecad:GFP
3D	w; Ecad:GFP/ Ecad:GFP
3E	w; Ecad:GFP/ Ecad:GFP
3F	w; Ecad:GFP/ Ecad:GFP
3G-I	NA
4A	w; Ecad:GFP/ Ecad:GFP
4B	w; Ecad:GFP/ Ecad:GFP
4C	w; Ecad:GFP/ Ecad:GFP
4D	w; Ecad:GFP/ Ecad:GFP
4E	w; Ubi-Ecad:GFP/ UAS-trbl; Act-Gal4, Ubi-GAL80^{ts} / +
4F	w; Ubi-Ecad:GFP/ UAS-trbl; Act-Gal4, Ubi-GAL80^{ts} / +
4G	w; Ubi-Ecad:GFP/ UAS-CycE^{18}; Act-Gal4, Ubi-GAL80^{ts} / UAS-CycE
4H	w; Ubi-Ecad:GFP/ UAS-CycE^{18}; Act-Gal4, Ubi-GAL80^{ts} / UAS-CycE
4I	w; Ecad:GFP/ Ecad:GFP w; Ubi-Ecad:GFP/ UAS-trbl; Act-Gal4, Ubi-GAL80^{ts} / + w; Ubi-Ecad:GFP/ UAS-CycE^{18}; Act-Gal4, Ubi-GAL80^{ts} / UAS-CycE
4J	w; Ecad:GFP /Ecad:GFP w; Ubi-Ecad:GFP/ UAS-trbl; Act-Gal4, Ubi-GAL80^{ts} / + w; Ubi-Ecad:GFP/ UAS-CycE^{18}; Act-Gal4, Ubi-GAL80^{ts} / UAS-CycE
5A	w; Ecad:3xGFP/+
5B	w; Ecad:3xGFP/+
5C	w; Ecad:3xGFP/+
5D	w; Ecad:3xGFP/+
5E	w; Ecad:3xGFP/+
5F	w; Ecad:3xGFP/+
5G	w; Ecad:3xGFP/+
5H	w; Ecad:3xGFP/+
6A	w, ban-nls:GFP; Ecad:3xmKate2/+ w; Ubi-nls:GFP /Ecad:3xmKate2
6B	w; Ecad:3xmKate2/+; Jub:GFP/+
6C	w, hs-flp; Ecad:3xmKate2/ UAS-jub^{dsRNA} ; Act>CD2>Gal4, UAS-Caax:tBFP/+
6D	w, hs-flp, sqh:3xGFP; Ecad:3xmKate2/ UAS-jub^{dsRNA}; Act>CD2>Gal4, UAS-Caax:tBFP/+
6E	w; Ecad:GFP/+; Pnr-Gal4/ UAS-Actn^{dsRNA} w; Ecad:GFP/+; Pnr-Gal4/ UAS-w^{dsRNA} w, hs-flp, sqh:3xGFP; Ecad:3xmKate2/+; Act>CD2>Gal4, UAS-Caax:tBFP/ UAS-Actn^{dsRNA} w, hs-flp, sqh:3xGFP; Ecad:3xmKate2/+; Act>CD2>Gal4, UAS-Caax:tBFP/ UAS-w^{dsRNA}
7A	w; Ecad:3xGFP/+; UAS-Tor^{dsRNA}/+
7B	w; Ecad:3xGFP/+; UAS-Tor^{dsRNA}/+
7C	w; Ecad:3xGFP/+; UAS-Tor^{dsRNA}/+
7D	N$^{l1N\text{-}ts1}$/Y; Ecad:3xGFP/+ w/Y; Ecad:3xGFP/+
7E	w; Ecad:3xGFP/+; NRE-nls:mChFP/+ w, Ubi-nls:RFP, FRT19A; Ecad:3xGFP/+
7F	w; Ecad:3xGFP/+; NRE-nls:mChFP/+ w, Ubi-nls:RFP, FRT19A; Ecad:3xGFP/+
7G	N$^{l1N\text{-}ts1}$/Y; Ecad:3xGFP/+ w/Y; Ecad:3xGFP/+
7H	N$^{l1N\text{-}ts1}$/Y; Ecad:3xGFP/+

	w/Y; Ecad:3xGFP/+
S1A	w; Ecad:GFP/ Ecad:GFP
S1B	w; Ecad:GFP/ Ecad:GFP
S1C	w; Ecad:GFP/ Ecad:GFP
S1D	w; Ecad:GFP/ Ecad:GFP
S1E	w; Ubi-PH:GFP,Ubi-His2B:RFP/+
S1F	w; Ecad:GFP/ Ecad:GFP
S2A	w; Ecad:GFP/ Ecad:GFP
S2B	w; Ecad:3xmKate2/+; Act-Gal4, Ubi-GAL80^{ts}/ UAS-GC3Ai w; Ecad:3xTagRFP/+; Act-Gal4, Ubi-GAL80^{ts}/ UAS-GC3Ai
S2C	w; Ecad:GFP/ Ecad:GFP
S2D	w, hs-flp; Ecad:3xGFP/ UAS-RHG^{dsRNA}; Act>CD2>Gal4, UAS-Caax:tBFP/+
S2E	w; Ecad:GFP/ Ecad:GFP
S2F	w; Ecad:GFP/ Ecad:GFP
S2G-J	w; Ecad:GFP/ Ecad:GFP
S2K	w; Ecad:GFP/ Ecad:GFP
S3A	w; Ecad:GFP/ Ecad:GFP
S3B	w; Ecad:GFP/ Ecad:GFP
S3C	w; Ecad:GFP/ Ecad:GFP
S3D	w, sqh:mTagRFP/w ; Act-Gal4, Ubi-GAL80^{ts}/+; UAS-GC3Ai/+ w, sqh:mTagRFP/w ; UAS-CycE^{18}/ Act-Gal4, Ubi-GAL80^{ts}; UAS-CycE/UAS-GC3Ai
S3E	w; Ubi-Ecad:GFP/ UAS-trbl; Act-Gal4, Ubi-GAL80^{ts} / + w; Ubi-Ecad:GFP/ UAS-CycE^{18}; Act-Gal4, Ubi-GAL80^{ts} / UAS-CycE
S4A	w; Ecad:3xGFP/+
S4B	w; Ecad:3xGFP/+
S4C	w; Ecad:3xGFP/+
S4D	w; Ecad:3xGFP/+
S4E	w; Ecad:3xmKate2/+; Act-Gal4, Ubi-GAL80^{ts}/ UAS-GC3Ai
S4F	w, hs-flp, ban-nls:GFP; Ecad:3xmKate2/+
S5A	NA
S5B	NA
S5C	w; Ecad:3xmKate2/+; Ubi-KTR:GFP/+
S5D	w; Ecad:3xmKate2/ UAS-Ras^{V12}; Ubi-KTR:GFP/ Act>CD2>Gal4, UAS-Caax:tBFP
S5E	w; Ecad:3xmKate2/+; Ubi-KTR:GFP/+
S5F	w, hs-flp, ban-nls:GFP; Ecad:3xmKate2/+
S5G	w; Ecad:3xmKate2/ Diap1$^{3.5}$-GFP w; Ecad:3xmKate2/ Ubi-nls:GFP
S5H	w, hs-flp; Ecad:3xmKate2/ UAS-jub^{dsRNA}; Act>CD2>Gal4, UAS-Caax:tBFP/ UAS-GC3Ai w, hs-flp, UAS-w^{dsRNA}; Ecad:3xmKate2/ +; Act>CD2>Gal4, UAS-Caax:tBFP/ UAS-GC3Ai
S5I	w, hs-flp; Ecad:3xmKate2/ UAS-jub^{dsRNA}; Act>CD2>Gal4, UAS-Caax:tBFP/+ w, hs-flp, UAS-w^{dsRNA}; Ecad:3xmKate2/ +; Act>CD2>Gal4, UAS-Caax:tBFP/ UAS-GC3Ai
S6A	w; Ecad:3xGFP/+; UAS-Tor^{dsRNA}/+
S6B	w; Ecad:3xGFP/+; UAS-Tor^{dsRNA}/+
S6C	w; azot^{KO}/azot^{KO}; Ubi-Ecad:GFP/ Ubi-Ecad:GFP w; +/+; Ubi-Ecad:GFP/ Ubi-Ecad:GFP
S6D	w; azot^{KO}/azot^{KO}; Ubi-Ecad:GFP/ Ubi-Ecad:GFP w; +/+; Ubi-Ecad:GFP/ Ubi-Ecad:GFP
S7A	N$^{l1N\text{-}ts1}$/Y; Ecad:3xmKate2/+; Ubi-2xpMagHigh1:AD, Ubi-Gal4DB:2xnMagHigh1/ UAS-GC3Ai w/Y; Ecad:3xmKate2/+; Ubi-2xpMagHigh1:AD, Ubi-Gal4DB:2xnMagHigh1/ UAS-GC3Ai
S7B	N$^{l1N\text{-}ts1}$/Y; Ecad:3xGFP/+ w/Y; Ecad:3xGFP/+
S7C	N$^{l1N\text{-}ts1}$/Y; Ecad:3xGFP/+ w/Y; Ecad:3xGFP/+
S7D	N$^{l1N\text{-}ts1}$/Y; Ecad:3xGFP/+ w/Y; Ecad:3xGFP/+
S7E	N$^{l1N\text{-}ts1}$/Y; Ecad:3xGFP/+ w/Y; Ecad:3xGFP/+w/Y; Ecad:3xGFP/+
S7F	w, hs-flp / UAS-Notch^{dsRNA}; Ecad:3xmKate2/+; Act>CD2>Gal4, UAS-Caax:tBFP/ Diap1$^{4.3}$-GFP w, hs-flp/ UAS-w^{dsRNA}; Ecad:3xmKate2/+; Act>CD2>Gal4, UAS-Caax:tBFP/ Diap1$^{4.3}$-GFP

	w, hs-flp, ban-nls:GFP/ UAS-Notch^{dsRNA}; Ecad:3xmKate2/+; Act>CD2>Gal4, UAS-Caax:tBFP/+ w, hs-flp, ban-nls:GFP/ UAS-w^{dsRNA}; Ecad:3xmKate2/+; Act>CD2>Gal4, UAS-Caax:tBFP/+
S7G	N$^{1N\text{-}ts1}$/Y; Ecad:3xGFP/+ w/Y; Ecad:3xGFP/+
S7H	w; Ecad:3xGFP/+ ; NRE-nls:mChFP/+
S7I	w; Ecad:3xGFP/+ ; NRE-nls:mChFP/+

Table S2. Pupa genotype for each figure panel. Related to Figure 1 to 7.

SUPPLEMENTAL REFERENCES

S1. Villars, A., Matamoro-Vidal, A., Levillayer, F., and Levayer, R. (2022). Microtubule disassembly by caspases is an important rate-limiting step of cell extrusion. Nat Commun *13*, 1–18. 10.1038/s41467-022-31266-8.

S2. Regot, S., Hughey, J.J., Bajar, B.T., Carrasco, S., and Covert, M.W. (2014). High-sensitivity measurements of multiple kinase activities in live single cells. Cell *157*, 1724–1734. 10.1016/j.cell.2014.04.039.

S3. López-Gay, J.M., Nunley, H., Spencer, M., di Pietro, F., Guirao, B., Bosveld, F., Markova, O., Gaugue, I., Pelletier, S., Lubensky, D.K., et al. (2020). Apical stress fibers enable a scaling between cell mechanical response and area in epithelial tissue. Science *370*. 10.1126/science.abb2169.